Light Metals 2013 *Edited by: Barry Sadler*
TMS (The Minerals, Metals & Materials Society), 2013

Effect of Cooling Rate on Iron-rich Intermetallic Phases in 206 Cast Alloys

K. Liu [1], X. Cao [1,2], X.-G. Chen [1]

[1] University of Québec at Chicoutimi, Saguenay, QC, Canada, G7H 2B1
[2] National Research Council Canada - Aerospace, Montreal, QC, Canada, H3T 2B2

Keywords: Al-Cu 206 cast alloy, cooling rate, iron-rich intermetallic phase, solidification

Abstract

The effect of cooling rate on the solidification characteristics of the iron-rich intermetallics in 206 cast alloys with iron contents up to 0.5 wt% was investigated. The iron-rich intermetallics were analyzed and characterized by using Scanning Electron Microscopy (SEM), Differential Scanning Calorimeter (DSC) and Thermal Analysis (TA). It was found that Chinese script α-Fe and platelet β-Fe phases are the two main iron-rich intermetallics up to 0.3 wt% Fe. With increasing cooling rate, the precipitate temperature increases for α-Fe but decreases for β-Fe and eventually the formation of the β-Fe will be completely suppressed. At 0.5 wt% Fe, two extra iron-rich intermetallics, Chinese script Al_m(FeMn) and platelet Al_3(FeMn) are experimentally observed. With increasing cooling rate, the Al_3(FeMn) or Al_6(FeMn) phases that precipitated at relatively low cooling rate can be replaced by Al_m(FeMn) and α-Fe. The critical cooling rate to effectively suppress the formation of the platelet β-Fe and obtain dominant Chinese script α-Fe or Al_m(FeMn) decreases with increasing iron level.

Introduction

Al-Cu 206 cast alloys have been widely used in automotive and aerospace industries. However, they usually require extremely low Fe contents, normally lower than 0.10-0.15% (all alloy compositions are in wt% unless indicated otherwise), significantly increasing the manufacturing costs and limiting their applications. Due to the extremely low solubility in solid Al (0.005% at 450°C) [1], iron usually precipitates as the iron-rich intermetallics during solidification [2-4]. They have been thought to be harmful to the mechanical properties, especially the platelet iron-rich phases due to their brittle features and stress concentration effect caused by the sharp shape. In order to improve mechanical properties, the platelet iron-rich intermetallics are usually modified into Chinese script phases, which have been thought to be less harmful to the mechanical properties due to the compact morphology. Increasing the cooling rate is considered to be one of the efficient methods to hinder the formation of the platelet iron-rich intermetallics in Al-Si cast alloys. Belmares-Perales *et al.* [5] found that the β-AlFeSi disappeared at both very low (< 0.1 K/s) and high (> 3.5 K/s) cooling rates. It was reported that higher cooling rate decreases the volume fraction of the iron-rich platelet phase but increases that of the Chinese script phase [6]. Sigworth *et al.* [7] pointed out that high cooling rate would help to uniformly distribute the iron-rich intermetallics and thus have less detrimental effect on the properties of the alloys.

However, little work about the influence of cooling rate on the formation of iron-rich intermetallics has been reported in Al-Cu 206 cast alloys. Kamga *et al.* [8] found that the platelet β-Fe can be largely depressed in 206 cast alloys at 0.3% Fe with a Si/Fe ratio of 1 at a moderate cooling rate although the accurate value of the cooling rate was not given. In addition, the phase selection among iron-rich intermetallics Al_3Fe, Al_6Fe and Al_mFe has been frequently encountered in the Al-Fe binary alloy system, such as AA1xxx alloys during Direct Chill (DC) casting [9]. However, the very limited investigations conducted recently have indicated the significant effect of cooling rate on the selection of the diverse iron-rich intermetallic phases in 206 alloys at a high iron level of 0.5% [4, 10, 11]. To better control the microstructures and optimize the mechanical properties of the 206 cast alloys, especially at a high iron level (up to 0.5%), the effect of the cooling rate on the formation of iron-rich intermetallics needs to be systematically investigated.

Experimental

Table I shows the chemical compositions of the experimental 206 cast alloys at 0.15%, 0.3% and 0.5% Fe.

Table I. Chemical compositions of the experimental 206 cast alloys used in this work

Nominal iron content	Alloy Code	Actual alloy compositions (wt%)					
		Cu	Fe	Si	Mn	Mg	Al
0.15	B11	4.59	0.15	0.09	0.11	0.27	Bal.
	B12	4.58	0.16	0.11	0.21	0.29	Bal.
	B21	4.59	0.16	0.19	0.11	0.27	Bal.
	B22	4.64	0.17	0.19	0.21	0.27	Bal.
	B33	4.58	0.14	0.31	0.28	0.29	Bal.
0.3	311	4.46	0.33	0.08	0.11	0.33	Bal.
	312	4.54	0.31	0.11	0.19	0.29	Bal.
	321	4.51	0.29	0.19	0.09	0.28	Bal.
	322	4.52	0.29	0.21	0.19	0.29	Bal.
	333	4.51	0.31	0.29	0.32	0.31	Bal.
0.5	511	4.60	0.49	0.09	0.11	0.32	Bal.
	522	4.61	0.49	0.19	0.22	0.32	Bal.
	551	4.62	0.50	0.48	0.10	0.28	Bal.
	515	4.64	0.51	0.09	0.53	0.31	Bal.

In each test, approximately 3 kg of material was prepared in a clay-graphite crucible by using an electric resistance furnace. The temperature of the melt was maintained at ~ 750°C for 30 minutes and the molten alloy was gently stirred to homogenize and avoid the entrainment of the surface oxide films during holding at 750°C. In order to cast the experimental alloys at various cooling rates, two methods have been used in this work. One was to pour the molten metal into a small preheated stainless steel crucible which was coated with a BN aerosol (Figure 1a). Then the samples were cooled to room temperature in compressed air with various pressures to reach different cooling rates (0.2, 1.4 and 2.0 K/s). The other method for higher cooling rates was to cast the samples directly into a wedge shaped copper mold that was

preheated to 250°C and also coated with a BN aerosol (Figure 1b). Three K-type thermocouples were located in positions A, B and C to record the variation of the temperature with time. The cooling rates at the A, B and C positions during solidification were calculated to be about 3.5, 5.0 and 7.5 K/s, respectively. In the present work, all the cooling rates were calculated based on the temperature difference over the solidification interval.

As is known, the cooling rate, particularly during slow cooling, can be accurately controlled in the Differential Scanning Calorimeter (DSC) test. Therefore, the DSC technique was used to investigate the effect of cooling rate on the phase selection of the iron-rich intermetallics in the 206 cast alloys at 0.5% Fe. The DSC samples were taken from the solidified Thermal Analysis (TA) cast ingots obtained at 0.2 K/s and then rapidly heated to 700°C at 2 K/s. After holding at 700°C for 5 minutes, the samples were then cooled at 0.02, 0.1, 0.2 and 1.0 K/s.

The samples were later mounted and polished for metallographic observations. The volume fraction of the iron-rich intermetallics was measured by using an optical microscope equipped with an image analyzer at a magnification of 500X. Scanning Electron Microscope (SEM) equipped with Electron Back-Scattered Diffraction (EBSD) pattern acquisition camera and Channel 5 software was used to identify the iron-rich intermetallic phases.

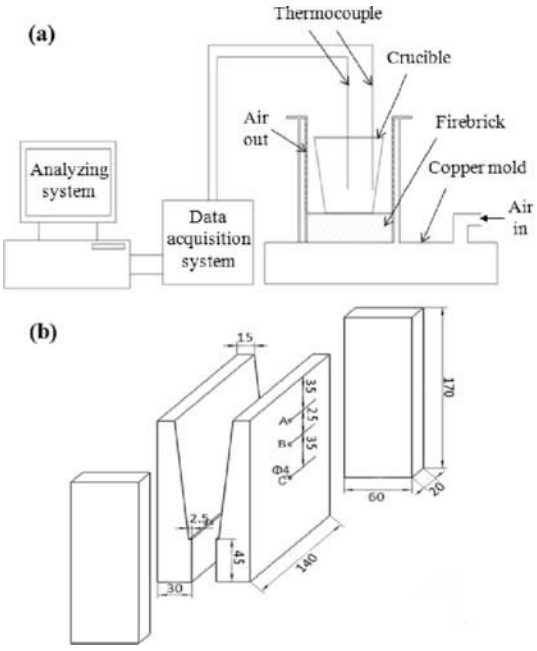

Figure 1. Schematic illustration for the molds used in this work

Results and discussion

1. Iron-rich intermetallics in 206 cast alloys solidified at 0.2 K/s

Figures 2a and 2b show two typical iron-rich intermetallics, i.e. platelet β-Fe ($Al_7Cu_2(FeMn)$) obtained in Alloy B11 (0.15% Fe) and Chinese script α-Fe ($Al_{15}(FeMn)_3(SiCu)_2$) in Alloy 333 (0.3% Fe) solidified at 0.2 K/s. EBSD was used to identify the iron-rich intermetallic phases and the results are shown in Figures 2c-2f. Figures 2c and 2e display the typical microimages of the iron-rich intermetallics while the corresponding simulated patterns are shown in Figures 2d and 2f.

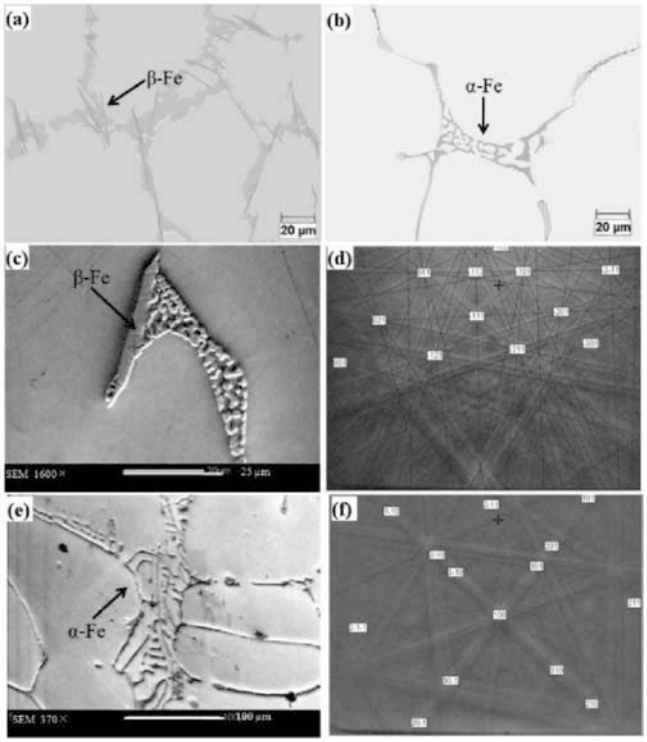

Figure 2. Typical iron-rich intermetallics in 206 cast alloys at 0.15% and 0.3% Fe and simulated EBSD results; (a, c, d) β-Fe from Alloy B11 (MAD=0.129), and (b, e, f) α-Fe from Alloy 333 (MAD=0.312)

In addition to β-Fe and α-Fe, two extra iron-rich intermetallics, i.e. Chinese script $Al_m(FeMn)$ and platelet $Al_3(FeMn)$ are obtained in the alloys at 0.5% Fe(Figures 3a and 3b). Two typical iron-rich intermetallics and their corresponding EBSD results are shown in Figures 3c-3f.

Both α-Fe and $Al_m(FeMn)$ have similar Chinese script morphology. The same is true for both platelet β-Fe and $Al_3(FeMn)$. However, these phases with similar morphologies can be clearly identified due to their different crystal structures and lattice parameters [10, 11]. In the EBSD results, the Mean Angular Deviation (MAD) between the experimental and the calculated patterns represents the accuracy of the solution given by the software (Channel 5). A smaller value indicates a closer match between the experimental and the simulated patterns. Normally, a MAD value lower than 0.7 is considered to be desirable for an accurate solution [12]. It was found that the MAD values for β-Fe and α-Fe are 0.129 and 0.312 (Figure 2), respectively while they are 0.238 for $Al_m(FeMn)$ and 0.215 for $Al_3(FeMn)$ (Figure 3), respectively. All these MAD values are much lower than 0.7 and thus confirms the presence of platelet β-Fe and Chinese script α-Fe in 206 cast alloys up to 0.3% Fe. At 0.5% Fe, however, both Chinese script $Al_m(FeMn)$ and platelet $Al_3(FeMn)$ are also present in addition to the β-Fe and α-Fe.

Figure 4 summarizes the volume percentage (Vol. %) of the iron-rich intermetallics in the experimental 206 cast alloys. It should be pointed out that the Vol.% of the β-Fe is calculated to be the difference between the total volume percentages of the

iron-rich intermetallics and the remaining iron-rich intermetallic phases (i.e. α–Fe, Al_m(FeMn) and Al_3(FeMn)). It was found that almost all the iron-rich intermetallics are β-Fe platelets in Alloys B11 and 311 but α-Fe for Alloys B33, 333 and 551. In Alloys B12, B21, B22, 312, 321 and 322, both α-Fe and β-Fe coexist in different proportions. In Alloys 511 and 522, Al_m(FeMn) is observed in addition to β-Fe while both platelet Al_3(FeMn) and β-Fe are found in Alloy 515.

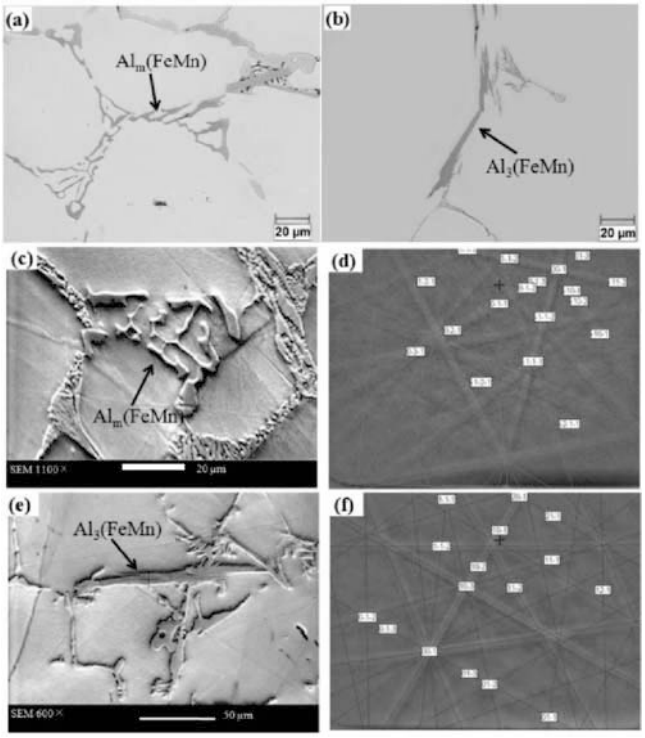

Figure 3. Typical iron-rich intermetallics in experimental 206 cast alloys at 0.5% Fe and the simulated EBSD results; (a, c, d) Al_m(FeMn) from Alloy 511 (MAD=0.238), and (b, e, f) Al_3(FeMn) from Alloy 515 (MAD=0.215)

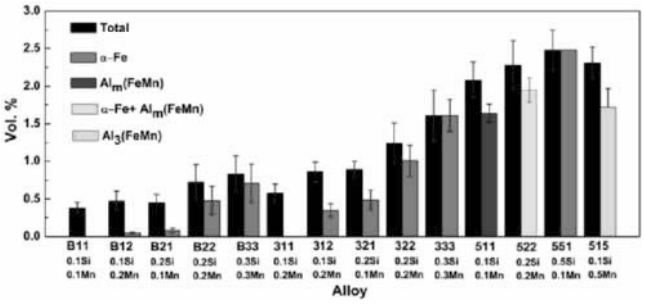

Figure 4. Vol.% of the iron-rich intermetallics obtained at a cooling rate of 0.2 K/s in experimental 206 cast alloys

2. Effect of cooling rate on the iron-rich intermetallic phases

2.1 Phase competition of iron-rich intermetallic phases at 0.15% and 0.3% Fe

As indicated in the previous studies [2, 3, 8] and the present work, it can be found that only two iron-rich intermetallic phases, i.e. α-Fe and β-Fe are present in 206 alloys at low iron levels (up to 0.3% Fe), as shown in Figure 4. Here, Alloys B22 and 322 are taken as two typical materials at 0.15% and 0.3% Fe, respectively, to characterize the effect of the cooling rate on the formation of the iron-rich intermetallics.

Figure 5 shows the microstructures of Alloys B22 and 322 solidified at 0.2 and 2.0 K/s. It is observed that both α-Fe and β-Fe coexist at 0.2 K/s (Figures 5a and 5c). At 2.0 K/s, however, only α-Fe is observed (Figures 5b and 5d), indicating that high cooling rate hinders the formation of the β-Fe phase.

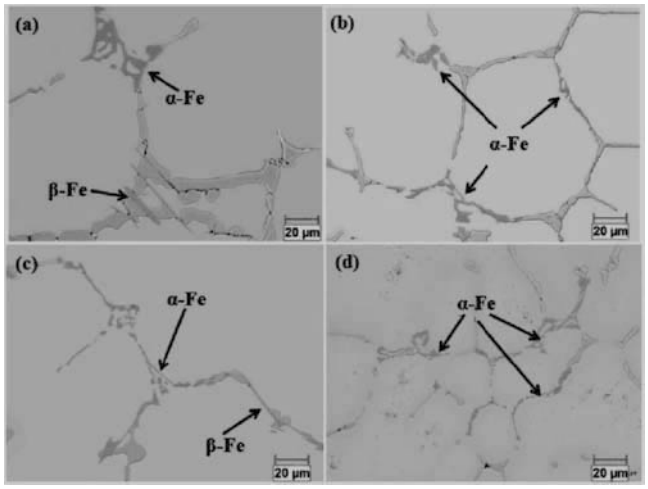

Figure 5. Microstructures of Alloys B22 (a, b) and 322 (c, d) at various cooling rates (0.2 K/s for a and c, 2.0 K/s for b and d)

DSC was also performed to verify the formation of the two intermetallic phases in Alloy B22. The heating curves in the enlarged zones for α-Fe and β-Fe [2, 3] using the cast samples obtained at different cooling rates are shown in Figure 6. It can be seen that the formation temperature and peak intensity of the β-Fe decrease with increasing cooling rate. Therefore, a higher cooling rate reduces the precipitation temperature and the volume percent of the β-Fe, i.e. hinders its formation, further confirming the optical observations as shown in Figure 5. In contrast, more α-Fe is formed at higher cooling rates (1.4 K/S and 2.0 K/S, as shown in Figure 6b). The peak intensity and formation temperature of the α-Fe phase increase with increasing cooling rate, indicating the promoting effect of the cooling rate on the formation of the α-Fe. Therefore, higher cooling rate increases the precipitation temperature and the volume percent of the α-Fe phase, i.e. favours the formation of the α-Fe phase.

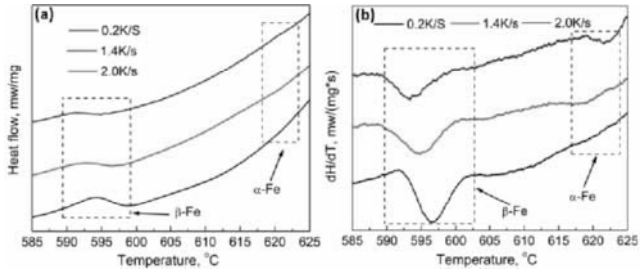

Figure 6. DSC heating curves (a) and their first derivatives (b) of Alloy B22 at various cooling rates

Figure 7 shows the TA cooling curves of Alloy 322 solidified at 0.2 K/s and 1.4 K/s. Similar to the DSC observation in Alloy B22 (Figure 6), it can be found that the peaks for both α-Fe and β-Fe are detected at 0.2 K/s, as shown in Figure 7a but the peak for β-Fe disappears at 1.4 K/s (Figure 7b), further confirming that the higher cooling rate can hinder the formation of the β-Fe. The formation temperature of the α-Fe is observed to increase with increasing cooling rate, as shown in Figure 7, indicating that higher cooling rate favours its formation.

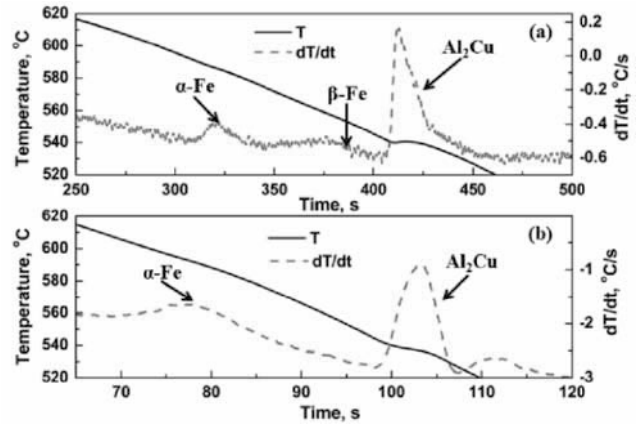

Figure 7. TA cooling curves and their first derivatives of Alloy 322 at cooling rates of (a) 0.2 K/s and (b) 1.4 K/s

As shown in Figures 6 and 7, the formation temperature decreases for β-Fe but increases for α-Fe with increasing cooling rates. Thus, α-Fe is easier to precipitate than β-Fe, particularly at high cooling rate. In addition, the formation temperature of α-Fe is higher than β-Fe [2, 3] and thus α-Fe precipitates earlier than β-Fe. The "early" formed α-Fe consumes part of element iron and thus the amount of free iron available for β-Fe is reduced. Furthermore, β-Fe phase precipitates at a temperature more close to the Al-Cu eutectic reaction at a higher cooling rate [3]. With the fine eutectic microstructure obtained at a higher cooling rate, the growth of β-Fe is also expected to be hindered and refined [5, 13]. Therefore, the formation of β-Fe is much more difficult at a high cooling rate.

Though the high cooling rate suppresses the formation of platelet β-Fe, the critical cooling rate to effectively hinder its formation varies with the alloy composition. Based on the results of the relative volume fraction of the α-Fe in the experimental 206 cast alloys at 0.15% and 0.3% Fe, casting process maps to correlate the iron-rich intermetallics to the cooling rate are established for the experimental alloys as shown in Figure 8. It was observed that the relative volume percent of the α-Fe phase increases with increasing cooling rate at a given alloy composition. For instance, the relative volume percent of α-Fe in Alloy 312 increases from 40% at 0.2 K/s to 85% at 1.4 K/s and 100% at 2.0 K/s. For a given alloy, there exists a threshold cooling rate above which β-Fe can be effectively suppressed. However, this critical cooling rate greatly depends on the alloy composition. For instance, the critical cooling rate is about 5 K/s for Alloy B21 but 2 K/s for Alloy B22 (Figure 8a), and 1.5 K/s for Alloy 321 but 0.5 K/s for Alloy 322 (Figure 8b). In addition, the highest peak is observed for Alloys B11 and 311, which have a dominant platelet β-Fe phase. And then the curve decreases with increasing alloy element additions. However, it is found that the curves at 0.3% Fe decreases faster than at 0.15% Fe, indicating that the critical cooling rate decreases more sharply at a higher iron level. For example, the critical cooling rate is extrapolated to be 9-10 K/s for Alloy B11 but decreases to about 7 K/s for Alloy 311. Similarly, it is about 5 K/s for Alloy B21 but about 1.4 K/s for Alloy 321, indicating that the critical cooling rate decreases with increasing iron level.

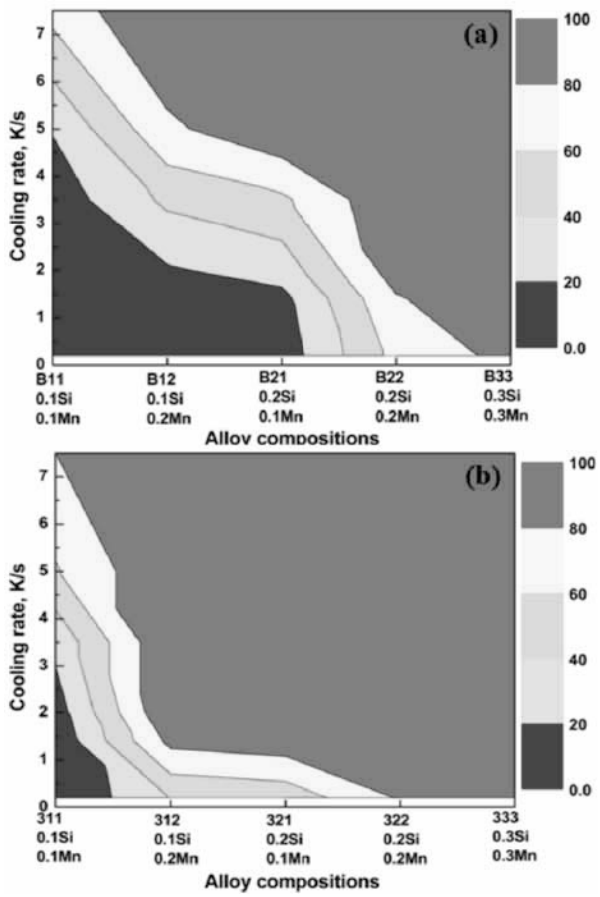

Figure 8. Relative volume percent of the α-Fe at various cooling rates at 0.15% Fe (a) and 0.3% Fe (b)

In summary, higher cooling rate promotes the formation of α-Fe but suppresses β-Fe and the critical cooling rate to effectively suppress the formation of β-Fe varies with alloy compositions at the iron content up to 0.3%. The threshold cooling rate decreases with increasing iron content.

2.2 Phase selection of iron-rich intermetallic phases at 0.5% Fe

When the iron content increases to 0.5%, two extra intermetallic phases, Al_m(FeMn) and Al_3(FeMn) are observed to precipitate in the 206 cast alloys in addition to the existing α-Fe and β-Fe phases, as revealed by the recent studies [4, 10, 11]. Therefore, it is important to clarify how the four iron-rich intermetallics solidify at various cooling rates. To this end, the effect of cooling rate on the phase selection among Al_m(FeMn), Al_3(FeMn), α-Fe and β-Fe in the alloys at 0.5% Fe has been addressed in the following section.

In this work, DSC was used to accurately control the cooling rate during solidification. The cooling curves of the samples solidified at various cooling rates for the four experimental alloys

at 0.5% Fe are shown in Figure 9, in which the arrow indicates the formation of the dominant iron-rich intermetallics (Al_m(FeMn), Al_3(FeMn) or α-Fe) while the formation of β-Fe is marked by the rectangles [4].

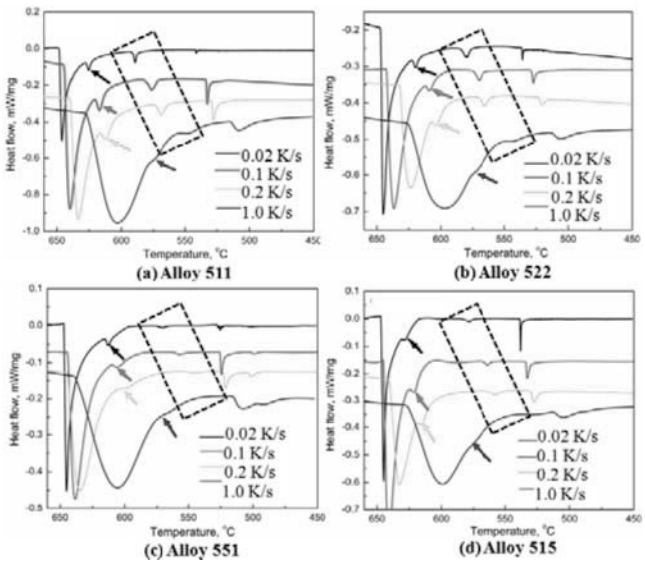

Figure 9. DSC cooling curves of the 206 alloys at 0.5% Fe solidified at various cooling rates

It can be seen that the formation temperature of the dominant iron-rich intermetallics (indicated by the arrows in Figure 9) decreases with increasing cooling rate. The peak intensity of the β-Fe (indicated by the rectangles in Figure 9) also decreases with increasing cooling rate. For instance, the peak intensity of β-Fe becomes so weak at 0.2 K/s and even disappears at 1.0 K/s in Alloy 551, confirming that the higher cooling rate suppress the formation of platelet β-Fe, similar to the results obtained at 0.15% and 0.3% Fe. It is also found that there is a critical cooling rate that effectively suppresses β-Fe at 0.5% Fe, which varies with the alloy composition. As shown in Figure 9, the peak intensity of β-Fe decreases in the order of Alloys 511, 522, 515 and 551 at 0.2 K/s while it disappears in Alloys 515 and 551 although it is still present in Alloys 511 and 522 at 1.0 K/s. However, it can be found that the critical cooling rate is much lower than that at 0.15% and 0.3% Fe. For instance, the critical cooling rate is about 1.0 K/s for Alloy 511 at 0.5% Fe, much lower than 9-10 K/s for Alloy B11 at 0.15% Fe and 7 K/s for Alloy 311 at 0.3% Fe (Figure 8). Therefore, it is much easier to suppress the formation of platelet β-Fe for the experimental 206 alloys at higher Fe contents. This further supports the conclusion drawn at 0.15% and 0.3% Fe, the critical cooling rate decreases with increasing iron content.

The dominant iron-rich intermetallics formed at various cooling rates have been identified by using EBSD [4] and the microstructures of Alloy 511 are shown in Figure 10 as a typical example. It can be found that the dominant iron-rich intermetallics will depend on the cooling rate, similar to AA1xxx [9]. For Alloy 511, the dominant iron-rich intermetallic is Al_3(FeMn) at 0.02 K/s, Al_6(FeMn) at 0.1 K/s and Al_m(FeMn) at 0.2-1.0 K/s. Table II summaries the dominant iron-rich intermetallics and their formation temperature solidified at various cooling rates at 0.5% Fe. It can be found that the formation temperature of the dominant iron-rich intermetallics decreases with increasing cooling rate. The types of the dominant iron-rich intermetallics appearing in the solidified structures will depend on the cooling rate, i.e. Al_3(FeMn) and Al_6(FeMn) appear at relatively low cooling rate while Al_m(FeMn) and α-Fe at high cooling rate.

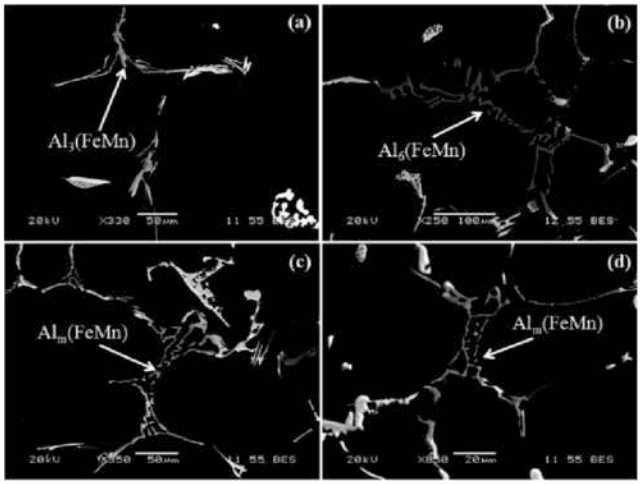

Figure 10. Microstructure of Alloy 511 at various cooling rates: (a) 0.02 K/s, (b) 0.1 K/s, (c) 0.2 K/s and (d) 1.0 K/s

Table II. Formation of main iron-rich intermetallic phases (MIP) at various cooling rates (Vc) in the alloys at 0.5% Fe

Vc (K/s)	Alloy 511		Alloy 522		Alloy 551		Alloy 515	
	MIP	T (°C)	MIP	T (°C)	MIP	T (°C)	MIP	T (°C)
0.02	3	625	3	619	3	611	6	627
0.1	6	616	6	608	α+m	605	6+3	621
0.2	m	612	m+α	603	α	602	3	615
1	m	581	m+α	576	α	573	m	577

Note: 3-Al_3(FeMn), 6-Al_6(FeMn) and m-Al_m(FeMn).

The effect of the cooling rate on intermetallic phase selection can be explained by the competitive growth model based on the growth temperature theory [9, 14]. The relationship between the growth temperature (T_G) and the cooling rate (V_C) is shown in the following equation [14, 15]:

$$T_G = T_{EU} - kV_C^{1/2} \quad (1)$$

Where T_{EU} is the equilibrium eutectic temperature of an iron-rich intermetallic phase and k is a constant. The value of k varies with the type of the iron-rich intermetallics. During phase selection, the iron-rich intermetallics with a higher growth temperature (T_G) will precipitate and grow preferentially and thus become the predominant intermetallic phase during solidification. The dominant phase can be replaced by another iron-rich intermetallic with a higher growth temperature.

As shown in Table II, Al_3(FeMn) is the first iron-rich intermetallic phase to form due to its high formation temperature in Alloys 511, 522 and 551. Then it is replaced by Al_6(FeMn) or Al_m(FeMn)/α-Fe with increasing cooling rate. In Alloy 515, the formation temperature of Al_6(FeMn) becomes the highest due to

the high Mn content [4] and then the precipitation of $Al_6(FeMn)$ is eventually replaced by $Al_3(FeMn)$ at 0.2 K/s and $Al_m(FeMn)$ at 1.0 K/s. In addition, it can be found that the dominant iron-rich intermetallics in the four experimental 206 cast alloys at 0.5% Fe are Chinese script $Al_m(FeMn)$/α-Fe at a cooling rate of 1 K/s or higher, which is lower than the industrial permanent mold casting condition (2-3 K/s), indicating the great potential to design and cast new 206 alloys at a high iron level.

3. Prospect of 206 cast alloys at a high iron level

In the present work, the effect of cooling rate on the 206 cast alloys at an iron level up to 0.5% has been studied. It is found that high cooling rate can promote the formation of Chinese script α-Fe or $Al_m(FeMn)$ but suppress the platelet β-Fe. There exists a critical cooling rate to effectively suppress the formation of the platelet β-Fe and obtain the dominant Chinese script α-Fe or $Al_m(FeMn)$. This threshold cooling rate decreases with increasing iron content. Particularly, this value can be easily reached in the industrial permanent mold casting condition for a well-designed and controlled alloy composition. For instance, the critical cooling rate is about 2 K/s for Alloy B22, 0.5 K/s for Alloy 322 and 0.2 K/s for Alloy 522, all being lower than the cooling rate experienced in industrial permanent mold casting (2~3 K/s). Therefore, Chinese script α-Fe or $Al_m(FeMn)$ can be predominantly obtained for all the experimental alloys solidified in normal industrial permanent mold casting. Due to the fact that the Chinese script morphology can minimize the harmful effect on the mechanical properties, the design and development of new 206 cast alloys at high iron contents may become feasible under well controlled solidification conditions, which will significantly reduce the costs of casting Al-Cu alloys by using recycled aluminum alloys and hence have potential to significantly expand the applications of the Al-Cu cast alloys in the automotive and aerospace industries.

Conclusions

(1) Both Chinese script α-Fe and platelet β-Fe phases are observed to be the two main iron-rich phases and can coexist in the solidified 206 alloys at an iron content up to 0.3%. In addition to the Chinese script α-Fe and platelet β-Fe, however, two extra iron-rich phases, i.e. Chinese script $Al_m(FeMn)$ and platelet $Al_3(FeMn)$ are experimentally observed at 0.5% Fe.

(2) With increasing cooling rate, the formation temperature increases for α-Fe but decreases for β-Fe and eventually the formation of platelet β-Fe can be completely suppressed, leading to the full precipitation of Chinese script α-Fe at an iron content of up to 0.3%.

(3) At 0.5% Fe, the formation of $Al_m(FeMn)$, α-Fe, $Al_3(FeMn)$ and $Al_6(FeMn)$ also depends on cooling rate. With increasing cooling rate, the formation temperature of each iron-rich intermetallic phase decreases. The $Al_3(FeMn)$ or $Al_6(FeMn)$ phases that precipitated at relatively low cooling rate can be replaced by $Al_m(FeMn)$ and/or α-Fe at high cooling rate. In addition, the formation of β-Fe is also found to be suppressed at a high cooling rate at 0.5% Fe.

(4) There exists a threshold cooling rate which depends on the alloy composition to effectively suppress the formation of platelet β-Fe and obtain the dominant Chinese script α-Fe or $Al_m(FeMn)$. This critical value decreases with increasing iron content. For all the experimental alloys up to 0.5% Fe, the critical cooling rate is lower than that used in industrial permanent mold casting condition, indicating the great potential to design and develop new 206 cast alloys at a high iron level.

Acknowledgements

The authors would like to acknowledge the financial support from the Natural Sciences and Engineering Research Council of Canada (NSERC) and Rio Tinto Alcan through the NSERC Industrial Research Chair in Metallurgy of Aluminum Transformation at the University of Québec at Chicoutimi.

References

1. N.A. Belov, A.A. Aksenov and D.G. Eskin, *Iron in aluminum alloys: impurity and alloying element* (London: Taylor & Francis, 2002), 3.
2. K. Liu, X. Cao and X.G. Chen. "Solidification of iron-rich intermetallic phases in Al-4.5Cu-0.3Fe cast alloy," *Metall. Mater. Trans. A*, 42 (2011), 2004-2016.
3. K. Liu, X. Cao and X.G. Chen. "Effect of Mn, Si and cooling rate on the formation of iron-rich intermetallics in 206 cast alloys," *Metall. Mater. Trans. B*, 43B (2012), 1231-1240.
4. K. Liu, X. Cao and X.G. Chen. "Formation and phase selection of iron-rich intermetallics in Al-4.6Cu-0.5Fe cast alloys," *Metall. Mater. Trans. A, online published, DOI:10.1007/s11661-012-1419-7*, (2012).
5. S. Belmares-Perales, et al. "Effect of cooling rate and Fe/Mn weight ratio on volume fractions of α-AlFeSi and β-AlFeSi phases in Al-7.3Si-3.5Cu alloy," *Met. Mater. Int*, 14 (2008), 307-314.
6. G. Gustafsson, T. Thorvaldssons and G.L. Dunlop. "The influence of Fe and Cr on the microstructure of cast Al-Si-Mg alloy," *Metall. Mater. Trans. A*, 17 A (1986), 45-52.
7. G.K. Sigworth, S. Shivkumar and D. Apelian. "The influence of molten metal processing on mechanical properties of cast Al-Si-Mg alloys," *AFS Trans.*, 97 (1989), 811-824.
8. H. Kamguo Kamga, et al. "Solidification of aluminum-copper B206 alloys with iron and silicon additions," *Metall. Mater. Trans. A*, 41 (2010), 2844-2855.
9. C.M. Allen, et al. "Intermetallic phase selection in 1XXX A1 alloys," *Prog. Mater. Sci.*, 43 (1998), 89-170.
10. K. Liu, X. Cao and X.G. Chen. "A new iron-rich intermetallic--AlmFe phase formed in Al-4.6Cu-0.5Fe cast alloy," *Metall. Mater. Trans. A*, 43 (2012), 1097-1101.
11. K. Liu, X. Cao and X.G. Chen. "Precipitation of iron-rich intermetallic phases in Al-4.6Cu-0.5Fe-0.5Mn cast alloy," *J. Mater. Sci.* , 47 (2012), 4290-4298.
12. M. Kral. "Identification of intermetallic phases in a eutectic Al-Si casting alloy using electron backscatter diffraction pattern analysis," *Scripta Mater.*, 51 (2004), 215-219.
13. L.A. Narayanan, F.H. Samuel and J.E. Gruzleski. "Crystallization behavior of iron-containing intermetallic compounds in 319 aluminum alloy," *Metall. Mater. Trans. A*, 25 (1994), 1761-1773.
14. D. Liang and H. Jones. "Effect of growth velocity on growth temperature of the Al-Al3Fe and Al-Al6Fe eutectics," *Z. Metallkde*, 83 (1992), 224-226.
15. R.M. Srivastava, et al. "Cooling rate evaluation for bulk amorphous alloys from eutectic microstructures in casting processes," *Metall. Trans.* , 43 (2002), 1670-1675.